

# Nonlinear Generation of Zonal Fields by the Beta-Induced Alfvén Eigenmode in Tokamak\*

ZHANG Huasen (张桦森)<sup>1</sup>, LIN Zhihong (林志宏)<sup>1,2</sup>

<sup>1</sup>Fusion Simulation Center, Peking University, Beijing 100871, China

<sup>2</sup>Department of Physics and Astronomy, University of California, Irvine, CA92697, USA

**Abstract** The zonal fields effect on the beta-induced Alfvén eigenmode (BAE) destabilized by the energetic particles in toroidal plasmas is studied through the gyrokinetic particle simulations. It is found that the localized zonal fields with a negative value around the mode rational surface are generated by the nonlinear BAE. In the weakly driven case, the zonal fields with a strong geodesic acoustic mode (GAM) component have weak effects on the nonlinear BAE evolution. In the strongly driven case, the zonal fields are dominated by a more significant zero frequency component and have stronger effects on the nonlinear BAE evolution.

**Keywords:** plasma Alfvén waves, plasma magnetohydrodynamics, plasma simulation

**PACS:** 52.35.Bj, 52.35.Mw, 52.55.Fa

**DOI:** 10.1088/1009-0630/15/10/02

## 1 Introduction

The Alfvén eigenmodes are a major concern in tokamaks because they can be easily destabilized by energetic particles through wave-particle interaction and cause the loss of the energetic particles. Among various Alfvén eigenmodes, the  $\beta$ -induced Alfvén eigenmode [1~4] (BAE) is due to the finite compressibility of the plasma pressure induced by the geodesic curvature of the equilibrium magnetic field. The BAE oscillates with the geodesic acoustic mode (GAM) frequency [5,6], which is of the order of the thermal ion transit frequency. Therefore, it has strong interaction with both the thermal ions and energetic particles. The BAE excitation has been widely observed in various tokamaks, such as Tore-Supra, ASDEX Upgrade and HL-2A, with ICRH, ECRH and tearing mode activities [7~12]. The fast frequency chirping of the BAE is also observed in tokamak experiments [13,14]. Meanwhile, the BAE has been intensively studied theoretically. It is found that the diamagnetic effects, elongation, and trapped particles can slightly shift the BAE continuum accumulation point [15]. The BAE damping effect and excitation threshold are also investigated [16,17]. The fully self-consistent simulations have also been applied to study the BAE linear excitation [18,19] and related nonlinear dynamics [20~22]. The zonal fields [23] are well known to play an important role in regulating the drift wave turbulence and reducing the saturation level [24]. The zonal fields can also be nonlinearly generated through Alfvén wave coupling, and in turn, affect the Alfvén wave saturation and nonlinear evolution. Recently, the generation of zonal fields by toroidal Alfvén eigenmode

(TAE) has been investigated theoretically [25,26]. The numerical simulation also shows that the zero frequency zonal fields may reduce the nonlinear TAE saturation level [27,28]. However, no self-consistent theory or simulation has been reported on the zonal fields generation by the nonlinear BAE coupling and their effects on the nonlinear BAE dynamics.

The gyrokinetic toroidal code (GTC) [24,29] has been successfully applied to the gyrokinetic simulation of TAE [30,31], RSAE [32~34], GAM [35,36], and BAE [19,22]. In particular, the fast and repetitive frequency chirping of the BAE is observed for the first time from the nonlinear gyrokinetic simulation [21]. In this work, we mainly focus on the generation of the zonal fields by the nonlinear BAE. It is found that, in the weakly driven case, the amplitude of the zonal fields is very low and has insignificant effects on the BAE saturation and nonlinear evolution. In the strongly driven case, the zonal fields can increase the initial BAE saturation amplitude. The radial mode structures of the zonal fields are quite similar between the weakly driven and the strongly driven cases, which have a negative value around the mode rational surface. By scanning the deviation from the BAE marginality, it is found that the nonlinear BAE with zonal fields is well located inside the marginality even at a large growth rate, which behaves different from the nonlinear BAE without zonal fields.

The paper is organized as follows: The simulation parameters are described in section 2. The simulation results are presented in section 3. Section 4 is the conclusion.

\*supported by the China Scholarship Council (No. 2009601135), the National Special Research Program of China for ITER (No. 2013GB111000), and the U. S. Department of Energy (DOE) SciDAC GSEP center

## 2 Simulation parameters

The BAE linear excitation properties and nonlinear evolution without zonal fields have been reported in our previous work [19~22]. In the current study, the generation of zonal fields by the nonlinear BAE will be investigated. In our simulation, the BAE is excited in a tokamak with concentric flux-surfaces. The radius profile of the safety factor  $q$  is  $q = 1.797 + 0.8(\psi/\psi_w) - 0.2(\psi/\psi_w)^2$ , where  $\psi$  is the poloidal flux function with  $\psi(r = 0) = 0$ ,  $\psi(r = a) = \psi_w$ , and  $a = 0.328R_0$  is the minor radius at the wall. The  $q = 2$  rational surface is located at a minor radius  $r_0 = 0.164R_0$  (Fig. 1(a)), where  $R_0$  is the major radius. Both thermal and energetic particles (EP) are protons with a Maxwellian velocity distribution and are treated using the nonlinear gyrokinetic equations [37], while electrons are treated as a massless fluid [29]. The temperature is uniform for all species with  $T_h = 12T_i$  and  $T_e = 0$ , where the subscript 'h', 'i' and 'e' denote the EP, thermal ions and electrons, respectively. Based on these parameters, the linear BAE frequency is  $\omega_0 = \sqrt{7/2}v_i/R_0$ , where  $v_i$  is the thermal ion velocity defined by  $v_i = \sqrt{2T_i/m_i}$ . The electron density  $n_0$  is uniform and the EP density profile is  $n_h = 0.07n_0 \times (1.0 + 0.2 \times (\tanh((0.24 - \psi/\psi_w)/0.1) - 1.0))$ , so that the EP density gradient has a maximum value of  $R_0/L_n \approx 7.8$  near  $q = 2$  surface, where  $L_n$  is the EP density gradient scale length (Fig. 1(b)). The thermal plasma beta at  $r_0$  is  $\beta = 8\pi n_0 T_i / B_0^2 = 0.0072$  with  $B_0$  being the on-axis magnetic field. Since the zonal fields are mostly generated by the nonlinear self-coupling of a single toroidal mode, the simulation treats a single toroidal mode number  $n = 3$ , which has  $k_\theta \rho_i = 0.044$  for  $R_0 = 838\rho_i$ . Here,  $k_\theta$  is the poloidal wavevector and  $\rho_i$  the thermal ion gyroradius. In our gyrokinetic simulation, both EP and thermal ion nonlinearities are retained to study the generation of zonal fields, while the electron fluid equations are kept linear. The effects

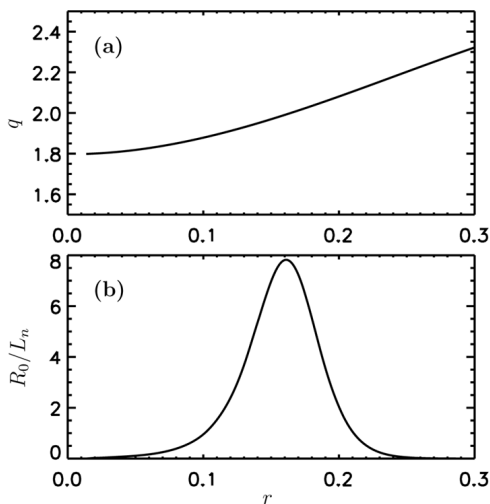


**Fig.1**  $q$  profile (a) and  $R_0/L_n$  profile (b) in radial direction

of the nonlinear terms in the electron fluid equations need to be further investigated. Since  $k_{\parallel} \sim 0$  for BAE, a filter is applied to keep only the  $m \in [nq - 2, nq + 2]$  poloidal harmonics to avoid the high  $k_{\parallel}$  noise. A slow sound approximation is used to suppress the ion acoustic wave (i.e.,  $E_{\parallel} = 0$ ). All perturbed quantities are set to be zero at the radial boundaries ( $r/R_0 = 0.048, 0.24$ ). By comparing the simulation results obtained with different grid numbers, it is found that the  $128 \times 512 \times 32$  grids in the radial ( $\psi$ ), poloidal ( $\theta$ ) and parallel ( $\zeta$ ) directions is refined enough to reach numerical convergence.

## 3 Simulation results

By varying the EP density gradient, the linear growth rate of the BAE is adjusted and the zonal fields are generated under two different linear growth rates, i.e.  $\gamma = 0.025\omega_0$  and  $\gamma = 0.06\omega_0$ . We denote the simulation with  $\gamma = 0.025\omega_0$  as the weakly driven case and the simulation with  $\gamma = 0.06\omega_0$  as the strongly driven case, respectively. Fig. 2 shows the nonlinear BAE evolution with and without zonal fields. In the weakly driven case (Fig. 2(a)), the zonal fields slightly suppress the initial saturation level but have little effects on the subsequent nonlinear BAE evolution. Since the zonal fields are generated by the thermal ion nonlinearity, the weakly driven simulations show that the thermal ion nonlinearity plays little role in the nonlinear BAE evolution near marginality, which agrees with our previous nonlinear BAE simulation results without zonal fields [22]. In the strongly driven case (Fig. 2(b)), the nonlinear BAE without zonal fields (black line in Fig. 2(b)) exhibits an amplitude oscillation with a repetitive downward frequency chirping similar to the results in Ref. [21]. However, the nonlinear BAE with zonal fields (blue line in Fig. 2(b)) has an even higher initial saturation level without repetitive frequency chirping. In later nonlinear stage, the nonlinear BAE amplitude exhibits a weak nonlinear oscillation and decreases to a level similar to the minimum saturation amplitude of the simulation without zonal fields. This result is different from the conventional understanding that the nonlinearly generated modes would usually increase the dissipation and reduce the saturation level [27]. The mechanisms for the zonal fields to increase the initial saturation level of the BAE will be investigated in our future work. The nonlinear simulation of the  $n = 3$  BAE with the  $n = 6$  sideband has also been performed to test the relative strength of the nonlinear coupling between different toroidal mode numbers. It is found that the nonlinear simulation result is almost the same as the simulation without the  $n = 6$  sideband. The  $n = 6$  sideband is not strongly generated due to the lack of the BAE resonant condition between different  $n$  modes. The zonal fields consist of the electric zonal field and the zonal current in our

simulation. To delineate the effects of the electric zonal field and the zonal current on the nonlinear BAE evolution, two controlled simulations are performed, i.e., one simulation is performed with the electric zonal field only and the other simulation is performed with the zonal current only. It is found that the zonal current has little effects on the nonlinear BAE evolution, the nonlinear BAE is mainly affected by the electric zonal field.

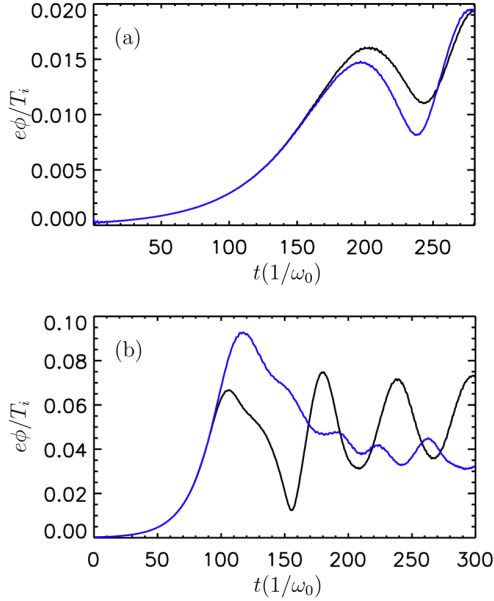


**Fig.2** Time evolution of the nonlinear BAE with and without zonal fields. Panels (a) and (b) are the simulations with linear growth rate  $\gamma = 0.025\omega_0$  and  $\gamma = 0.06\omega_0$ , respectively. The blue and black lines are simulation with and without zonal fields, respectively (color online)

The time evolution of the electric zonal field  $E_r$  is shown in Fig. 3 for the weakly driven and the strongly driven cases. A steady negative  $E_r$  with some fast oscillations is localized around the  $q = 2$  mode rational surface in both of the simulations. The frequency of the rapid  $E_r$  oscillation is consistent with the GAM frequency [5]. Comparing the Fig. 3(a) and (b), we can see that the maximum electric zonal field amplitude in the strongly driven case is one order of magnitude higher than that in the weakly driven case. In the weakly driven case (Fig. 3(a)), the electric zonal field with a GAM component is not strongly generated and has little effects on the nonlinear BAE dynamics. In the strongly driven case (Fig. 3(b)), the electric zonal field has a significant zero frequency component at the beginning of the BAE saturation ( $t \approx 110/\omega_0$ ), where the BAE amplitude reaches the maximum. In the later nonlinear stage ( $t > 150/\omega_0$ ), the BAE amplitude decreases to half of the initial saturation level. The zero frequency electric zonal field also decreases and the GAM oscillations become more significant. These results may indicate that the nonlinear BAE is mainly affected by the zero frequency electric zonal field and the GAM component plays little role in the nonlinear BAE evolution.

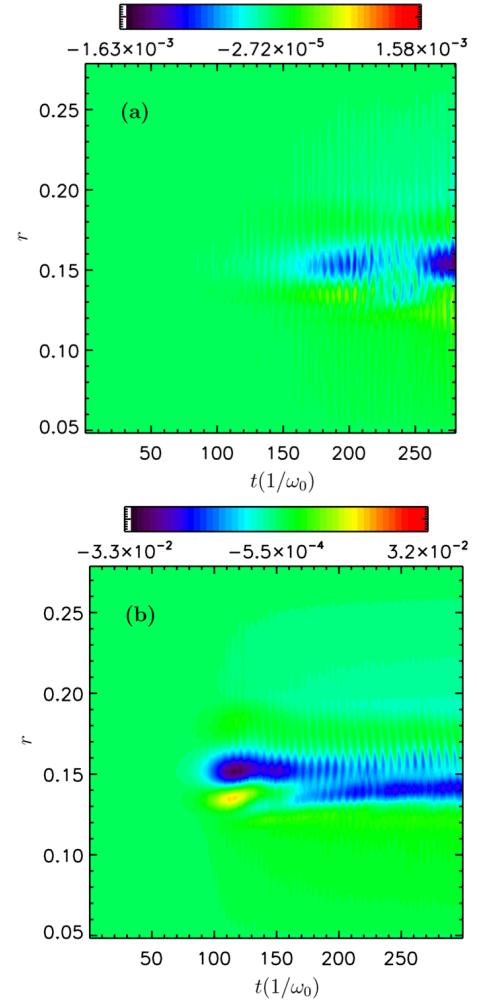


**Fig.3** Time ( $t$ ) evolution of the electric zonal field  $E_r$  in radial ( $r$ ) direction. Panels (a) and (b) are the simulations with linear growth rate  $\gamma = 0.025\omega_0$  and  $\gamma = 0.06\omega_0$ , respectively (color online)

The radial mode structure of the electric zonal field is shown in Fig. 4 for both the weakly driven (panel (a)) and strongly driven (panel (b)) cases. The mode structures are taken around the initial saturation stage for both simulations. We can see that the radial mode structures are quite similar between the two simulations. The electric zonal field is negative in value and locates slightly inside of the  $q = 2$  mode rational surface. The electric zonal field becomes positive at both the inner and outer sides of the BAE mode envelope. The amplitude of  $E_r$  in the weakly driven case is much lower than that in the strongly driven case, which may explain why the zonal fields have little effect on the nonlinear BAE dynamics in the weakly driven case.

Finally, the linear growth rate of the BAE is varied by changing the EP density gradient and the deviations from the BAE marginality are compared between the simulations with and without zonal fields (Fig. 5). For the simulations without zonal fields, the square of the BAE saturation amplitude  $(e\delta\phi/T_i)^2$  is proportional to the linear growth rate when  $\gamma/\omega_0 < 0.05$ , while there is no strong dependence when  $\gamma/\omega_0 > 0.05$ , which is well

deviated from the marginality. This result is consistent with our previous BAE study [22]. For the simulations with zonal fields, the saturation amplitudes are quite similar to the simulation results without zonal fields when  $\gamma/\omega_0 < 0.05$ , which further indicates that the zonal fields have little effect on the nonlinear BAE when  $\gamma/\omega_0 < 0.05$ . However, the zonal fields increase the BAE initial saturation level when  $\gamma/\omega_0 > 0.05$  in the simulation with zonal fields. The  $(e\delta\phi/T_i)^2$  is proportional to  $\gamma/\omega_0$  even for large linear growth rate, which shows that the zonal fields keep the nonlinear BAE well locating inside the marginality.

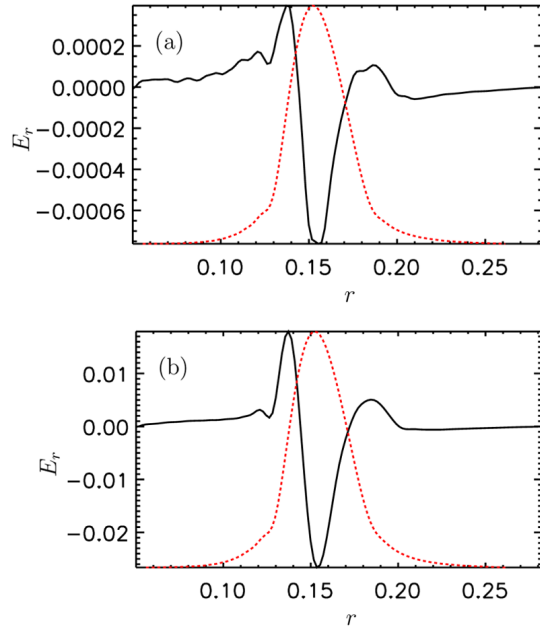


**Fig.4** The radial mode structure of the  $E_r$  at the initial saturation stage. Panels (a) and (b) are taken at  $t = 187/\omega_0$  in the weakly driven case and  $t = 112/\omega_0$  in the strongly driven case, respectively. The dotted red line is the radial mode structure of the BAE (color online)

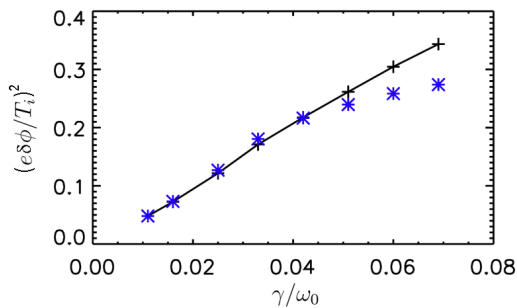


**Fig.5** The square of the saturation amplitude  $(e\delta\phi/T_i)^2$  vs linear growth rate. The '+' symbol denotes the simulation with zonal fields, while the '\*' symbol denotes the simulation without zonal fields (color online)

## 4 Conclusion

In this work, the gyrokinetic particle simulations are carried out to study the nonlinear BAE with zonal

fields. We find that the zonal fields with a strong GAM component have effects on the BAE saturation and nonlinear evolution in the weakly driven case. In the strongly driven case, the large BAE amplitude generates a more significant zero frequency zonal fields, which increase the BAE initial saturation amplitude. The radial mode structure of the zonal fields is localized with a negative value around the mode rational surface. By scanning the deviation from the BAE marginality, it is found that the nonlinear BAE with zonal fields is well located inside the marginality even for large linear growth rate. It should be noted that the nonlinear terms in the electron fluid equations are removed in our simulation, which may affect the generation of the zonal fields. The simulation with all the nonlinear terms will be investigated in our future work.

## Acknowledgements

Simulations were performed using supercomputers at ORNL, NERSC, and NSCC-TJ.

## References

- 1 Turnbull A D, Strait E J, Heidbrink W W, et al. 1993, Phys. Fluids B, 5: 2546
- 2 Chu M S, Greene J M, Lao L L, et al. 1992, Phys. Fluids B, 4: 3713
- 3 Heidbrink W W, Strait E J, Chu M S, et al. 1993, Phys. Rev. Lett., 71: 855
- 4 Heidbrink W W, Ruskov E, Carolipio E M, et al. 1999, Phys. Plasmas, 6: 1147
- 5 Winsor N, Johnson J L, and Dawson J M. 1968, Phys. Fluids, 11: 2448
- 6 Zonca F, Chen L, and Santoro R. 1996 Plasma Phys. Controlled Fusion, 38: 2011
- 7 Sabot R, Macor A, Nguyen C, et al. 2009, Nucl. Fusion, 49: 085033
- 8 Guimaraes-Filho Z O, Elbeze D, Sabot R, et al. 2011 Plasma Phys. Controlled Fusion, 53: 074012
- 9 Garcia-Munoz M, Fahrbach H U, Gunter S, et al. 2009, Phys. Rev. Lett., 100: 055005
- 10 Elfimov A G, Galvao R M O, Garcia-Munoz M, et al. 2011, Plasma Phys. Controlled Fusion, 53: 025006
- 11 Chen W, Ding X T, Liu Y, et al. 2011, Nucl. Fusion, 51: 063010
- 12 Chen W, Ding X T, Yang Q W, et al. 2010, Phys. Rev. Lett., 105: 185004
- 13 Classen I G J, Lauber P, Curran D, et al. 2011, Plasma Phys. Controlled Fusion, 53: 124018
- 14 Lauber P, Classen I G J, Curran D, et al. 2012, Nucl. Fusion, 52: 094007
- 15 Lauber P, Brudgam M, Curran D, et al. 2009, Plasma Phys. Controlled Fusion, 51: 124009
- 16 Bondeson A and Chu M S. 1996, Phys. Plasmas, 3: 3013
- 17 Nguyen C, Garbet X, and Smolyakov A I. 2008, Phys. Plasmas, 15: 112502

- 18 Wang X, Zonca F, and Chen L. 2010, Plasma Phys. Controlled Fusion, 52: 115005
- 19 Zhang H S, Lin Z, Holod I, et al. 2010, Phys. Plasmas, 17: 112505
- 20 Wang X, Zonca F, and Chen L. 2012, Phys. Rev. E, 86: 045401
- 21 Zhang H S, Lin Z, and Holod I. 2012, Phys. Rev. Lett., 109: 025001
- 22 Zhang H S, Lin Z, Deng W, et al. 2013, Phys. Plasmas, 20: 012510
- 23 Hasegawa A, Madennan C G, and Kodama Y. 1979, Phys. Fluids, 22: 2122
- 24 Lin Z, Hahm T S, Lee W W, et al. 1998, Science, 281: 1835
- 25 Chen L and Zonca F. 2012, Phys. Rev. Lett., 109: 145002
- 26 Qiu Z, Chen L, and Zonca F. 2013, Europhysics Letters, 101: 35001
- 27 Todo Y, Berk H L and Breizman B N. 2010, Nucl. Fusion, 50: 084016
- 28 Todo Y, Berk H L and Breizman B N. 2012, Nucl. Fusion, 52: 094018
- 29 Holod I, Zhang W L, Xiao Y, et al. 2009, Phys. Plasmas, 16: 122307
- 30 Nishimura Y. 2009, Phys. Plasmas, 16: 030702
- 31 Zhang W L, Holod I, Lin Z, et al. 2012, Phys. Plasmas, 19: 022507
- 32 Deng W, Lin Z, Holod I, et al. 2010, Phys. Plasmas, 17: 112504
- 33 Deng W, Lin L, Holod I, et al. 2012, Nucl. Fusion, 52: 043006
- 34 Spong D A, Bass E M, Deng W, et al. 2012, Phys. Plasmas, 19: 082511
- 35 Zhang H S, Qiu Z, Chen L, et al. 2009, Nucl. Fusion, 49: 125009
- 36 Zhang H S and Lin Z. 2010, Phys. Plasmas, 17: 072502
- 37 Brizard A J and Hahm T S. 2007, Rev. Mod. Phys., 79: 421

(Manuscript received 9 April 2013)

(Manuscript accepted 3 June 2013)

E-mail address of ZHANG Huasen:  
zhang.huasen@gmail.com